2014

Mitochondrial genome linearization is a causative factor for cardiomyopathy in mice and Drosophila

Yun Chen
Washington University School of Medicine in St. Louis

Megan Sparks
Washington University School of Medicine in St. Louis

Poonam Bhandari
Washington University School of Medicine in St. Louis

Scot J. Matkovich
Washington University School of Medicine in St. Louis

Gerald W. Dorn
Washington University School of Medicine in St. Louis

ANTIOXIDANTS & REDOX SIGNALING
Volume 21, Number 14, 2014

DOI: 10.1089/ars.2013.5432

Therapeutics

FORUM ORIGINAL RESEARCH COMMUNICATION

Mitochondrial Genome Linearization Is a Causative Factor for Cardiomyopathy in Mice and *Drosophila*

Yun Chen, Megan Sparks, Poonam Bhandari, Scot J. Matkovich, and Gerald W. Dorn II

Abstract

Aims: Mitofusin (Mfn)2 redundantly promotes mitochondrial outer membrane tethering and organelle fusion with Mfn1, and uniquely functions as the mitochondrial receptor for Parkin during PTEN-induced putative kinase 1 (PINK1)-Parkin-mediated mitophagy. Selective deletion of Mfn2 with retention of Mfn1 preserves mitochondrial fusion while rendering damaged mitochondria resistant to normal quality control culling mechanisms. Consequently, neuron and cardiomyocyte-specific Mfn2 gene ablation is associated with accumulation of damaged mitochondria and organ dysfunction. Here, we determined how mitochondrial DNA (mtDNA) damage contributes to cardiomyopathy in Mfn2-deficient hearts. ***Results:*** RNA sequencing of Mfn2-deficient hearts revealed increased expression of some nuclear-encoded mitochondrial genes, but mitochondrial-encoded transcripts were not upregulated in parallel and mtDNA content was decreased. Ultra-deep sequencing of mtDNA showed no increase in single nucleotide mutations, but copy number variations representing insertion–deletion (in–del) mutations were induced over time by cardiomyocyte-specific Mfn2 deficiency. Double-strand mtDNA breaks in the form of in–dels were confirmed by polymerase chain reaction, and in the form of linear mitochondrial genomes were identified by southern blot analysis. Linearization of *Drosophila* cardiomyocyte mtDNA using conditional cardiomyocyte-specific expression of mitochondrial targeted *Xho*I recapitulated the cardiomyopathy of Mfn2-deficient mouse hearts. ***Innovation:*** This is the first description of mitochondrial genome linearization as a causative factor in cardiomyopathy. ***Conclusion:*** One of the consequences of interrupting mitochondrial culling by the PINK1-Mfn2-Parkin mechanism is an increase in mtDNA double-stranded breaks, which adversely impact mitochondrial function and DNA replication. *Antioxid. Redox Signal.* 21, 1949–1959.

Introduction

Mitochondrial dynamics encompasses organelle motility, fission, and fusion. Subcellular mitochondrial transport and remodeling of highly interconnected mitochondrial networks through fusion and fission reactions is observed in most cell types (39). Fragmentation of these mitochondrial networks through organelle fission and network regeneration *via* organelle fusion are necessary to distribute mitochondria to daughter cells during cell mitosis (5). Because cardiomyocyte mitochondria exist as tightly packed and immobile organelles rather than as an interconnected network, and since adult cardiomyocytes have exited the mitotic cycle, these cells do not exhibit the typical requirement for mitochondrial dynamism. Indeed, despite having the largest proportion of mitochondria (~30% by volume) of any cell type, mitochondrial fusion has not been directly observed in adult cardiomyocytes (15). Nevertheless, cardiomyocytes express mitochondrial fusion and fission proteins in abundance, suggesting that there may be noncanonical functions for mitochondrial dynamics factors in this cell type.

In adult hearts, interruption of cardiomyocyte mitochondrial fusion by conditional combined genetic ablation of mitofusins (Mfn)1 and 2 not only induces mitochondrial fragmentation from unopposed mitochondrial fission, but provokes massive accumulation of abnormal mitochondria (12). Individual deletion of Mfn1 or Mfn2 in cardiac myocytes avoids mitochondrial fragmentation because these two proteins are functionally redundant fusion factors (15, 16). Nevertheless, cardiomyocyte Mfn2 deletion (but not Mfn1

Department of Internal Medicine, Center for Pharmacogenomics, Washington University School of Medicine, St. Louis, Missouri.

Innovation

Mitochondria are purportedly generated through biogenesis and undergo cyclic fusion and fission that maintains homeostasis until senescent or damaged organelles are eliminated by mitophagy. Here, we unify these three apparently distinct processes by describing a novel consequence of interrupted mitophagy due to ablation of mitofusin 2: mitochondrial DNA (mtDNA) linearization. We prove that mtDNA linearization is sufficient to cause cardiomyopathy in fruit flies. We propose that nuclear and mitochondrial biogenic programs do not supply new organelles, but instead produce replacement components for functioning mitochondria as they endlessly cycle between organelle renewal *via* fusion and elimination of dysfunctional components segregated *via* asymmetric fission.

deletion) provoked development of unusually large dysmorphic mitochondria, cardiomyocyte respiratory dysfunction, and progressive cardiomyopathy (9). The mechanistic basis by which Mfn2 (but not Mfn1) deficiency evokes accumulation of abnormal mitochondria was revealed through its selective ablation in mouse livers, hearts, and neurons (9, 26, 31, 33). Together, these studies describe a central role for Mfn2 in mitochondrial quality control as the essential transduction factor mediating signaling from the mitochondrial PTEN-induced putative kinase 1 (PINK1) to the cytosolic E3 ubiquitin ligase Parkin. Given that mitochondrial fusion is preserved when only one Mfn is ablated and the other is retained, the uniquely deleterious effects of Mfn2 ablation on mitochondrial structure and function appear to be explained by interruption of Parkin-mediated mitophagy.

Among the many potential molecular casualties of defective mitochondrial quality control is DNA of mitochondrial genomes (mitochondrial DNA [mtDNA]). Mitochondria possess ~16.6 kb circular genomes encoding 13 genes of the respiratory chain, plus essential ribosomal and transfer RNAs (tRNAs). Increased mtDNA point mutations and insertion–deletions (in–dels) have been implicated in skeletal myopathy caused by combined ablation of Mfn1 and Mfn2 (8), but in view of the recent identification of an essential function for Mfn2 in mitophagic mitochondrial culling it is unclear whether mtDNA damage occurred as a consequence of defective mitochondrial fusion or interruption of mitophagy. Accordingly, we interrogated mitochondrial genomes before and after appearance of the cardiomyopathy induced by cardiomyocyte-specific *Mfn2* gene deletion (9). In contrast to the point mutations that accumulated with mitochondrial fragmentation provoked by combined deletion of Mfn1 and Mfn2 in skeletal muscle, we observed no increase in mtDNA point mutations induced by cardiomyocyte-specific Mfn2 deficiency. We did, however, detect an increase in double-stranded mtDNA breaks manifested both as in–del mutations and linearized genomes, which were associated with loss of cardiac mtDNA. Because linearization of circular mtDNA has not previously been described in cardiomyopathy and its functional implications were unknown, we conditionally expressed a mitochondrial-targeted single cutting DNA restriction enzyme (*Xho*I) in *Drosophila* heart tubes. In the fruit fly heart, mtDNA linearization decreased mtDNA content and caused cardiomyopathy. These studies show that double-stranded mtDNA breaks linearize a fraction of mitochondrial genomes that, independent of mtDNA point or in–del mutations, can contribute to end-organ dysfunction.

Results

mtDNA defects in Mfn2-deficient hearts

Mfn2 is the essential mitochondrial receptor for Parkin on depolarized mitochondria (9, 26). Thus, Mfn2 deficiency produced by cardiac-specific gene ablation interrupts a protective mitophagy pathway, and the resulting accumulation of abnormal mitochondria impairs cardiomyocyte respiration and induces a progressive cardiomyopathy by 16 weeks of age (9). One of the molecular hallmarks of cardiomyopathy is altered cardiac gene expression (17), but the genetic response to interruption of Mfn2-facilitated cardiac mitophagy has not been described. Accordingly, we used deep RNA sequencing (28) to quantify expression of both nuclear- and mitochondrial-encoded mRNAs before (*i.e.*, in 6-week-old mice) and after (*i.e.*, in 16-week-old mice) onset of cardiomyopathy that develops in Mfn2-deficient mouse hearts. Genome-wide transcriptional profiling identified 7290 cardiac transcripts expressed at levels of one mRNA copy per cell or greater (raw sequence results were deposited at https://submit.ncbi.nlm.nih.gov/subs/bioproject/, project number SRX285687). Comparison of mRNA expression levels for 6 and 16 week Mfn2-deficient mouse hearts to their respective age-matched controls identified 1141 dysregulated (1.3-fold change from control, false discovery rate [FDR] = 0.01) cardiac-expressed mRNAs (Supplementary Table S1; Supplementary Data are available online at www.liebertpub.com/ars). Unsupervised hierarchical clustering of raw (Fig. 1A, left) or normalized (Fig. 1A, right) mRNA expression levels perfectly segregated control from Mfn2-deficient hearts. Sixteen-week-old Mfn2-deficient hearts tended to cluster to the right of their 6-week-old Mfn2 null counterparts, suggesting more severe mRNA dysregulation. Indeed, the number of regulated mRNAs changed more than 50%, 75%, or 100% was significantly greater in 16 week than 6 week Mfn2 null hearts (Chi-square $p < 0.001$ for each comparison). Thus, the transcriptional signature evoked by cardiomyocyte-specific Mfn2 deletion precedes cardiomyopathy and is exaggerated with age. Gene-ontology analysis revealed that a disproportionate number of the dysregulated transcripts belong to functional categories related to mitochondria or metabolism ($p < 0.05$; Fig. 1B), suggesting a primary effect of Mfn2 ablation on cardiac genes involving cellular metabolism.

Mitochondria contain ~800 nuclear-encoded and just 13 mitochondrial-encoded proteins (21). Of 766 nuclear-encoded mitochondrial proteins listed in www.mitoproteome.org, we detected 650 expressed at 1 mRNA copy per cell or greater in mouse hearts. A disproportionate 28% (183/650; compared to 1141/7290, or 16% of total cardiac transcripts; $p = 0.01$) of these cardiac mitochondrial protein encoding transcripts were dysregulated in Mfn2-deficient hearts (Fig. 1C and Supplementary Table S2). Modulated expression of mitochondrial genes anticipated cardiomyopathy, as it was detected in 6-week-old Mfn2 null hearts.

Mitochondrial biogenesis is frequently described in heart disease as reactive changes in the expression of genes that direct mtDNA replication and transcription (20, 40). We examined the mRNA expression profile induced by cardiomyocyte

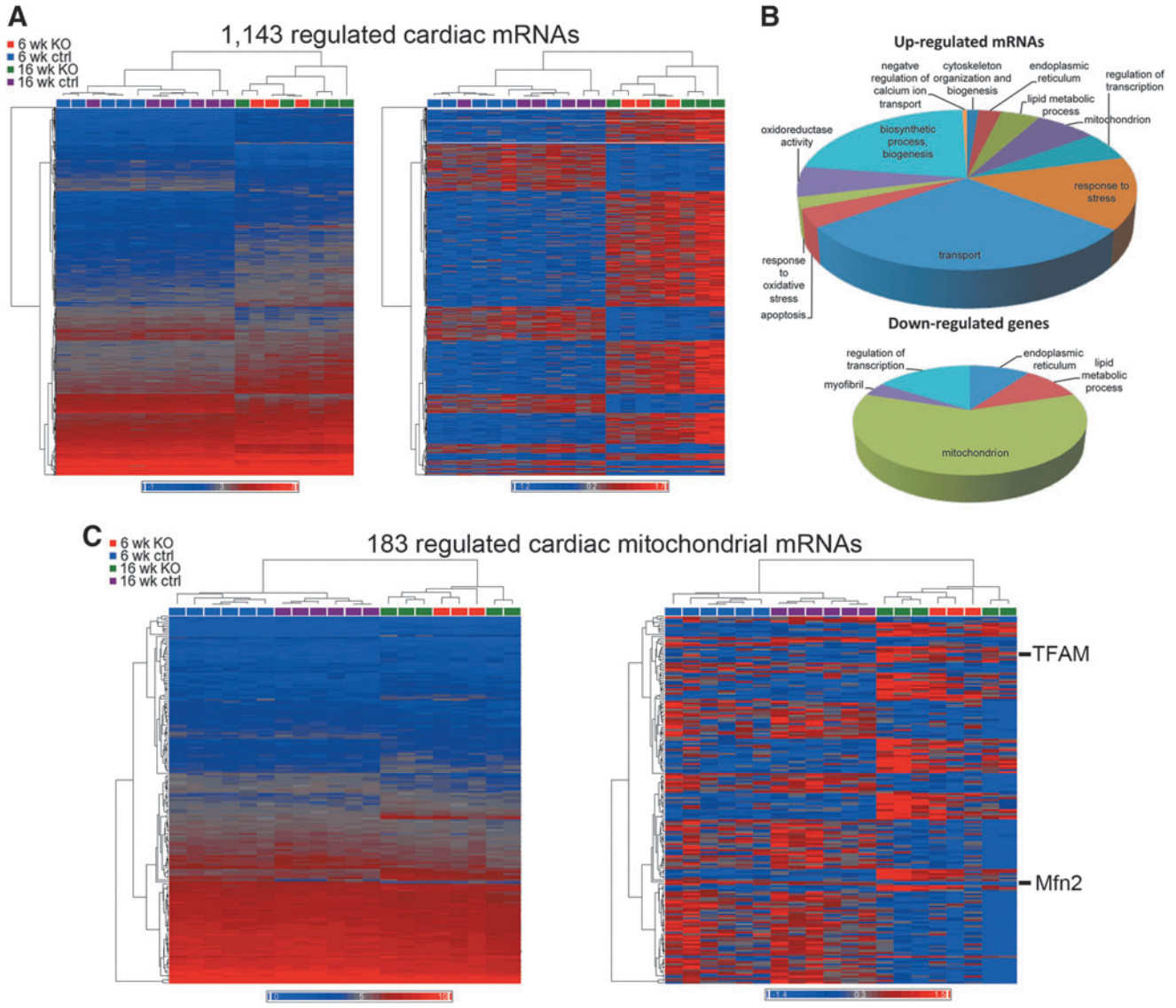

FIG. 1. Altered gene expression in Mfn2-deficient mouse hearts. (A) Heat map showing unsupervised nonhierarchical clustering of regulated mRNA expression levels in 6- and 16-week-old wild-type (ctrl) and *Myh6*-Cre Mfn2 KO hearts. Each column is a different mouse heart; each row is a different mRNA transcript. *Left panel* shows raw expression values, *right panel* shows same expression data normalized for each mRNA. Blue is fewer copies/cell, and red is greater copies/cell. **(B)** Gene Ontology classification of Mfn2-regulated mRNAs. **(C)** Unsupervised nonhierarchical clustering heat map of mRNA levels for 183 regulated mitochondrial genes. *Left panel* shows raw mRNA values, *right panel* is normalized data. Upregulated *TFAM* and downregulated *mfn2* (the KO gene) are indicated. Mfn, mitofusin; KO, knockout.

Mfn2 deficiency for regulated expression of mRNAs encoding factors central to mtDNA replication and RNA transcription. Expression of several nuclear-encoded mitochondrial biogenesis genes was increased only in 16-week-old Mfn2-deficient hearts (Fig. 2A). Remarkably, increased expression of some mtDNA replication and transcription factor genes concomitantly occurred with a precipitous decline in the levels of mtDNA relative to nuclear DNA (Fig. 2B, left) and loss of cardiomyocyte mitochondrial nucleoids (Fig. 2B, middle and right). We hypothesized that increased expression of nuclear-encoded mitochondrial genes was an attempt to compensate for the loss of mitochondrial genomes. Consistent with this notion, levels of the 13 mtDNA-derived transcripts did not increase in parallel with their nuclear-encoded mitochondrial protein counterparts, pointing to a primary failure of mitochondrial gene transcription (Fig. 2C). The loss of cardiac mtDNA content, upregulation of some nuclear-encoded mitochondrial transcription and replication factors, and absence of similar upregulation of mitochondrial-derived transcripts reveal a primary mtDNA defect in Mfn2-deficient hearts. A similar decrease in mtDNA has been observed in Mfn1/Mfn2 double knockout skeletal muscle (8). Since mitochondrial fusion is impaired by combined Mfn1/Mfn2 ablation, but not when Mfn2 is deleted alone, our findings suggest that the mitochondrial genomic defects accrue from interruption of Mfn2-Parkin-mediated mitophagy, and not abrogation of mitochondrial fusion.

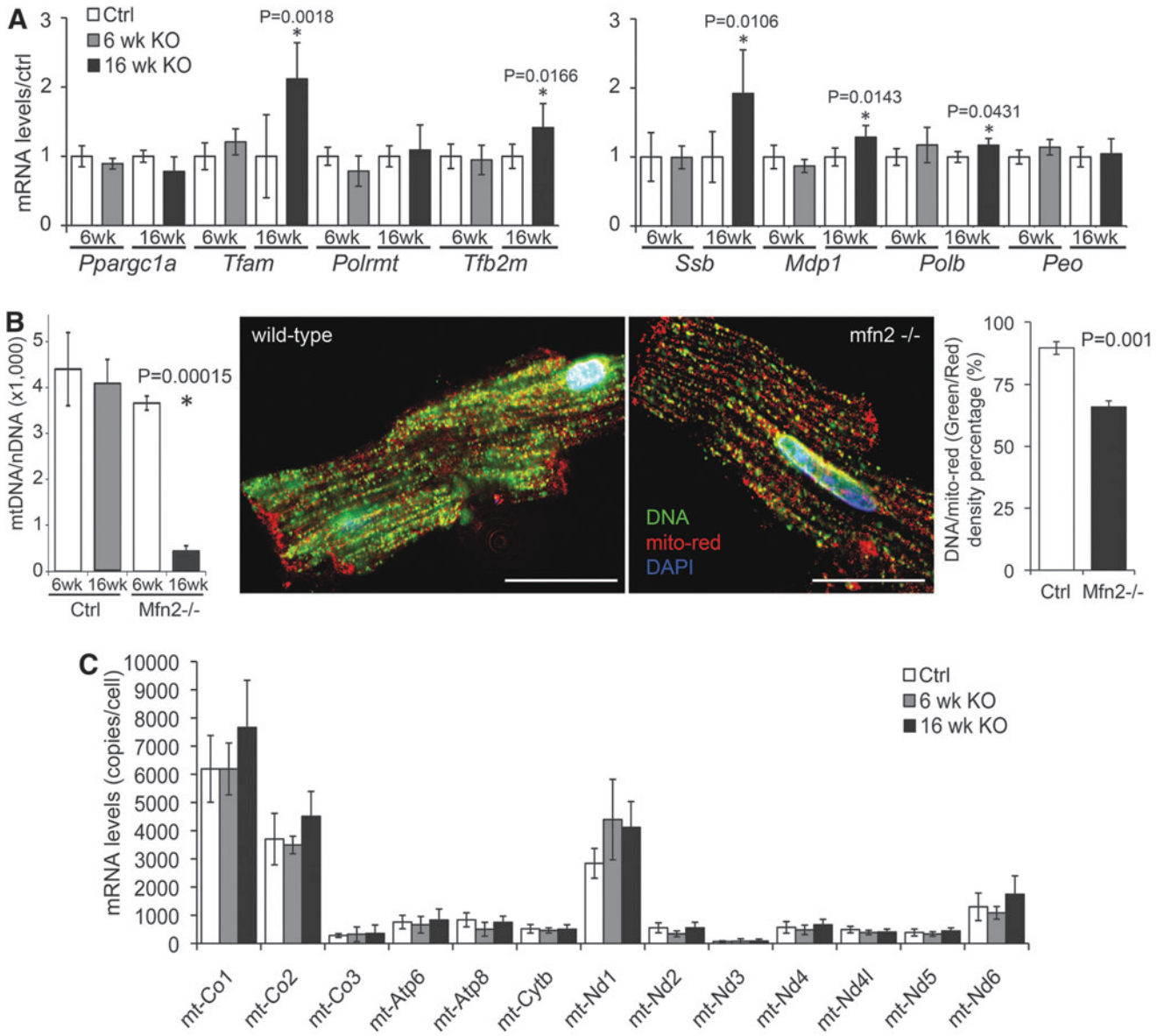

FIG. 2. Mitochondrial gene expression and mtDNA abnormalities in Mfn2-deficient mouse hearts. (A) mRNA levels, relative to same-age control, of nuclear-encoded mitochondrial transcription factors (left) and replication factors (right) taken from RNA-Seq data in Figure 1. *, Significantly different than age-matched controls by group *t*-test; *p*-Values are given on graphs. **(B)** Cardiomyocyte mitochondria lose mtDNA: (left) qPCR quantitation of mitochondrial-encoded *ND2* gene indexed to nuclear-encoded *Pecam* gene; $n=10$ per group; (middle) merged confocal analysis of mitochondrial nucleoid content: left, cardiomyocyte is from 16 week wild-type control and right, cardiomyocyte is from 16 week *Myh6*-Cre Mfn2 KO. Red is mito-tracker red, green is anti-dsDNA, nuclei are counterstained blue with DAPI. Mitochondrial nucleoids are visible as small yellow/green punctae within red mitochondria. White scale bar is 20 μm. Quantitative data ($n=3$ hearts per group) are to the right. **(C)** mRNA levels of each of the 13 mitochondrial genome-encoded mitochondrial proteins are not changed in Mfn2 KO hearts. mtDNA, mitochondrial DNA; qPCR, quantitative polymerase chain reaction.

Mitochondrial genomic rearrangements are caused by cardiac Mfn2 ablation

Combined ablation of Mfn1 and Mfn2 in skeletal muscle is postulated to induce skeletal myopathy in part by increasing mtDNA point and in–del mutations (8). We assessed the integrity of mitochondrial genomes in Mfn2-deficient mouse hearts by ultra-deep mtDNA resequencing. Because we estimated that mouse myocardium contains ~4000 mitochondrial genomes for each nuclear genome (Fig. 2B), to assure adequate coverage for mutation detection we resequenced myocardial mitochondrial genomes (Fig. 3A) at an average depth of 101,035±10,180 times per individual mouse heart. There were no differences in the frequency of common or rare single-nucleotide sequence variants between wild-type and Mfn2 knockout hearts: mtDNA polymorphisms (defined as variations from the reference sequence having a frequency of 1% or greater) were similar in wild-type and Mfn2-deficient hearts, as expected since polymorphisms tend to be consistent within a given mouse strain (2) (median 72 in wild-type, 66 in

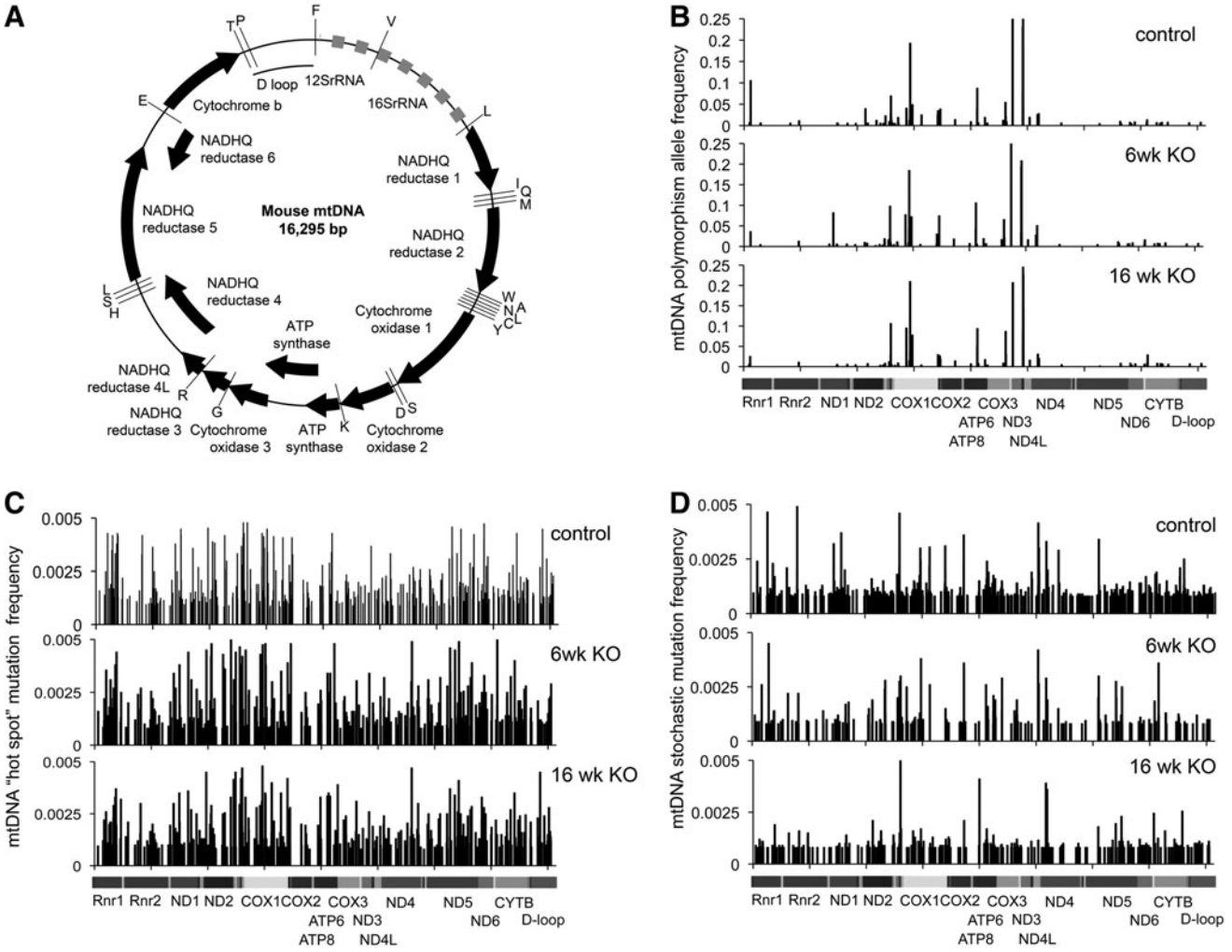

FIG. 3. Cardiac Mfn2 deficiency is not associated with increased myocardial single-nucleotide mtDNA sequence variations. (A) Schematic representation of murine mitochondrial genome. Mitochondrial-encoded genes are shown as *arrows* showing direction of transcription; tRNAs are indicated by their single letter amino acid coding. **(B)** Frequency and position of common polymorphic (allele freq >0.01) nucleotide variations in pooled 6 week ($n=4$) and 16 week controls ($n=3$), 6 week Mfn2 KO ($n=3$), 16 week Mfn2 KO ($n=3$) hearts. **(C)** Prevalence and position of rare variants in mutational "hot spots," that is, positions where mutations were detected in half of the same sequenced samples. **(D)** Frequency and position of rare mutations outside of mutational hot spots in the same samples as **(C)**. The distribution of mutations among protein-coding genes, tRNAs, rRNAs, and the D-loop control sequence was the same between genotypes. tRNA, transfer RNA; rRNA, ribosomal RNA.

Mfn2-deficient, Mann–Whitney $p=0.15$; Fig. 3B). We also found no difference in the frequency or distribution of rare mtDNA mutations, either within 966 bp of sequence defined as mtDNA mutational hot spots (median 344 mutations in controls, 350 in 6 weeks knockout (KO), and 323 in 16 weeks KO; $p=0.82$, Kruskal–Wallis test; Fig. 3C) or the remaining mtDNA sequence (median 137 variants in controls, 98 in 6 weeks KO, and 101 in 16 weeks KO; $p=0.92$, Kruskal–Wallis test; Fig. 3D). Single-nucleotide mutation frequency was similar within mtDNA encoding proteins, ribosomal RNA (rRNA), tRNA, and in the D-loop transcriptional control region (not shown).

mtDNA single nucleotide mutations are well tolerated, even at high frequencies (37), and so their contribution to mitochondrial dysfunction is likely small. By contrast, regional mtDNA in–dels that remove critical portions of mitochondrial genes are an established cause of disease (34). We therefore examined our mtDNA sequence data for evidence of in–dels, detectable as regional sequence copy number variations (CNV). In control hearts (6 and 16 week), sequence depth was fairly constant across mtDNA regions (Fig. 4A and Supplementary Fig. S1A). Sequence depth was also similar in 6-week-old Mfn2-deficient mtDNA, revealing no evidence of CNV (Supplementary Fig. S1A). Remarkably, some mtDNA sequences from 16-week-old Mfn2-deficient mouse hearts revealed discrete areas where sequence depth was significantly less (*i.e.*, diverging more that two standard deviation [SD]) than the mean control depth, identifying discrete genomic deletions (29) (Fig. 4A and Supplementary Fig. S1B–D). We confirmed that mtDNA deletions occurred only in 16-week-old Mfn2-deficient hearts in an independent cohort of samples analyzed by flanking polymerase chain reaction (PCR) analyses (Fig. 4B).

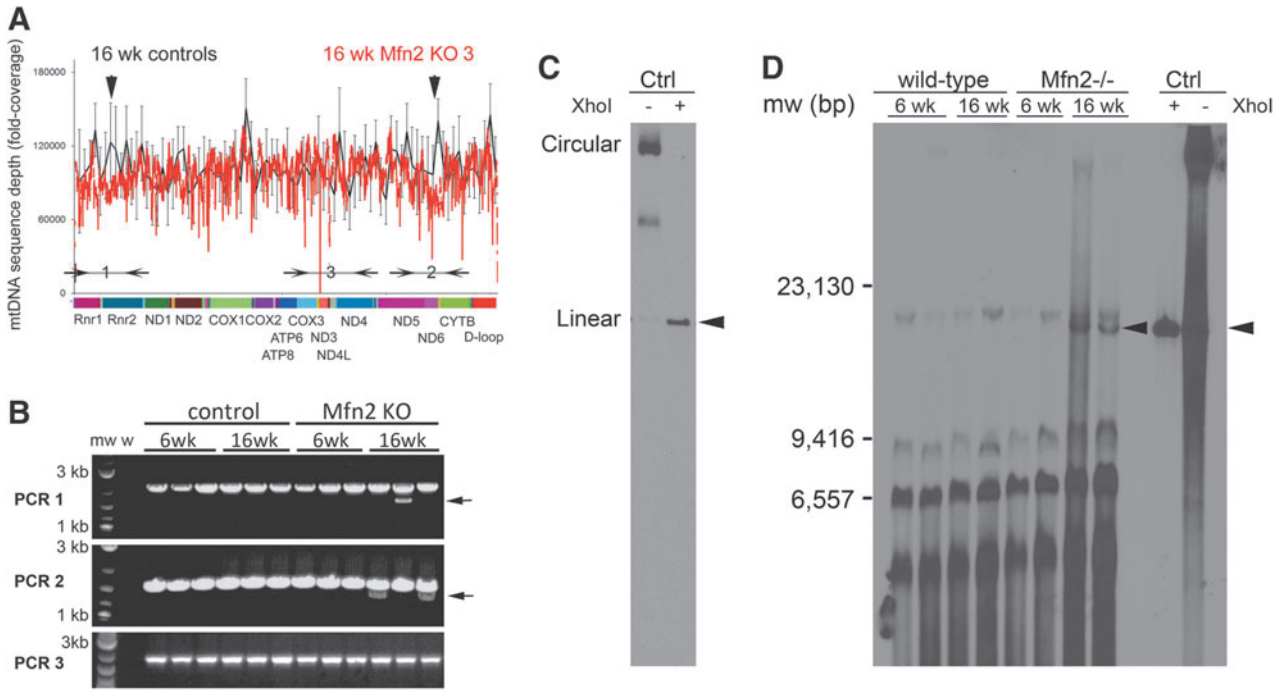

FIG. 4. Accumulation of mtDNA double-strand breaks in Mfn2-deficient hearts. (A) Sequence depth for mtDNA sequencing, depicted by nucleotide position across the mitochondrial genome, for the mean of all 16 week control hearts (black) and one of three 16 week Mfn2 KO hearts (red). Mitochondrial-encoded genes from Figure 3A are shown in their relative position along the horizontal axis. *Arrowheads* at top indicate two regions of CNV in the 16 week Mfn2 KO sequence. *Horizontal arrows* at the bottom show positions of PCR primers used for amplifying across CNV in **(B)**. Other mtDNA sequence data are depicted in Supplementary Figure S1. **(B)** Accumulation of regional mtDNA deletions in older Mfn2 KO hearts. PCR primers that span mitochondrial genome CNVs detected by sequencing **(A)** were used for 12 additional independent cardiac mtDNA samples. mtDNA deletions (*arrows*) were detected in all three 16 week Mfn2 KO hearts. **(C)** Linear mitochondrial genomes are detected in older Mfn2 KO hearts. Southern blotting of *Xho*I-linearized mitochondrial-specific mouse heart DNA. **(D)** Representative (of four per group) Southern blot analysis of mtDNA. Linear genomes are indicated with *arrowheads*. *Xho*I-cut mouse cardiac mtDNA is shown on the right (Ctrl). Intact circular mtDNA is not visualized, but equal DNA loading is shown by the faster-migrating nonspecific DNA signals. CNV, copy number variation; PCR, polymerase chain reaction.

Linear mitochondrial genomes accumulate in cardiac Mfn2 deficiency

A specific mtDNA deletion can cause disease when it deletes a critical portion of an encoded mtRNA, and when it is maternally transmitted and therefore ubiquitous throughout the organism (34). This cannot be the case with the mtDNA deletions we detected in Mfn2-deficient hearts as the causative cardiomyocyte-specific genetic intervention (*mfn2* gene ablation) spares the germ cells, and the mtDNA deletions we detected accumulate over time. Further, as revealed by the mtDNA sequence data, deletions appeared stochastically at multiple sites across the mitochondrial genomes, including within a single heart. Thus, these mtDNA in–del mutations almost certainly exhibit marked heteroplasmy, that is, a mixture of mutant and normal mitochondria within the same cell, and cannot explain the marked mitochondrial abnormalities observed in Mfn2-deficient mouse hearts (23). Accordingly, we looked for another explanation.

We considered that genomic mtDNA deletions require at least two distinct breaks in the circular double-stranded mtDNA (to delete part of the genome), followed by mtDNA re-circularization and strand repair. By this reasoning, linearization of mtDNA (the inevitable consequence of a single double-strand DNA break) is an absolute precondition for forming in–del mtDNA mutations. The effects of mtDNA linearization have not been studied in metazoan mitochondrial dysfunction. In yeast (which have branched linear mitochondrial genomes), double-stranded breaks are either repaired or the damaged genomes are cleared (19, 27). A similar quality control mechanism likely repairs or eliminates linear metazoan mtDNA. Since mtDNA linearization is a prerequisite for mtDNA deletions, their accumulation in older Mfn2-deficient hearts (vide supra) and Mfn1/Mfn2 double knockout skeletal muscle (8) links the putative mtDNA quality control mechanism to Mfn2-mediated mitochondrial culling.

We developed a gel electrophoresis/mtDNA-specific southern blot procedure to detect linear mtDNA in *in vivo* heart samples. First, we demonstrated that electrophoresis of intact and *Xho*I-treated mouse mtDNA (*Xho*I cuts mtDNA at a single site, thus linearizing it) on 0.5% agarose gels for 20 h at 60 V separates linear from intact circular mtDNA; linear mtDNA migrates faster (Fig. 4C). We then adapted this southern blotting approach to total DNA (*i.e.*, combined mitochondrial and nuclear DNA) extracted from mouse myocardium. Linear mtDNA from heart samples co-migrates with *Xho*I-cut mtDNA, and was detected in 16-week-old, but not

6-week-old, Mfn2-deficient hearts or control hearts (Fig. 4D, right; arrowheads). Because the experimental samples used whole heart (mixed nuclear and mitochondrial) DNA and we took precautions not to physically damage mtDNA by shearing, intact circular mtDNA is not visualized in the myocardial samples. It is therefore not possible to quantify the proportion of mtDNA that is linear *versus* nonlinear from this experiment. Nevertheless, the high concordance between heart samples with evidence for mtDNA linearization and mtDNA in–del mutations shows that a consequence of cardiac Mfn2 deficiency is accumulation of mtDNA with double-stranded breaks.

mtDNA linearization is sufficient to cause mitochondrial cardiomyopathy

The consequences of mtDNA linearization on cardiac homeostasis are unknown. Since we did not detect either mtDNA deletion mutations or linear mtDNA in normal hearts, we considered that normal mtDNA repair mechanisms efficiently re-circularize the linearized mitochondrial genomes or selectively eliminate them, with few cumulative adverse effects. However, the putative mtDNA re-circularization and repair mechanisms may be overwhelmed and mitochondrial integrity compromised when mtDNA damage is severe and/or normal mitophagic clearance mechanisms are suppressed. To test these possibilities we developed *Drosophila* models conditionally expressing mitochondrial-targeted *Xho*I in cardiomyocytes (Mito*Xho*I). As with mouse mtDNA (Fig. 4C), *Xho*I cleaves *Drosophila* mtDNA at a single site (in the cytochrome oxidase subunit 1 gene) (38), linearizing mtDNA without deleting any of the mitochondrial genome. Expression of pUAS-Mito*Xho*I using a conventional cardiomyocyte-specific tincΔ4Gal4 driver (Fig. 5A, left) resulted in almost universal lethality during the second and third instar larval stages and early after pupation. Two escapers that emerged as adults showed severely impaired cardiac function assessed by optical coherence tomography (OCT) (Fig. 5A, right), and these flies almost immediately succumbed. Thus, cardiomyocyte-specific Mito*Xho*I expression established that linear mtDNA is incompatible with normal

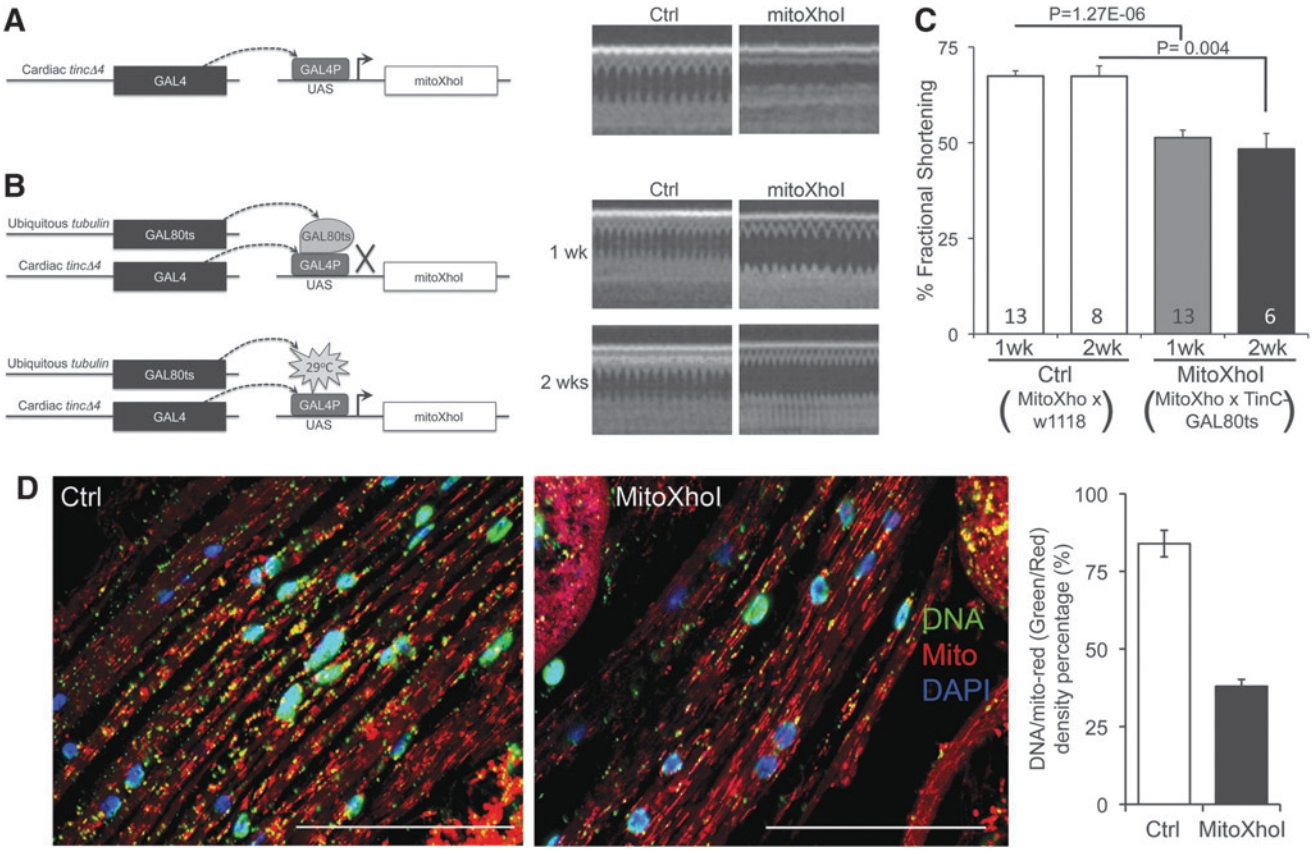

FIG. 5. mtDNA linearization with Mito*Xho*I induces cardiomyopathy in *Drosophila*. (A) (left) Schematic depiction of conventional TincD4-Gal4/pUAS system for cardiac-specific expression of Mito*Xho*I in *Drosophila* that was >99% lethal before emergence as adults. (right) OCT of a control (Ctrl) and one of two adult cardiac Mito*Xho*I flies; heart tube function is severely depressed in the Mito*Xho*I fly. **(B)** (left) Schematic diagram of temperature inducible system for transient, conditional expression of Mito*Xho*I in fly cardiomyocytes. (right) Representative OCT of control and conditional Mito*Xho*I heart tubes 1 week (top) and 2 weeks (bottom) after induction. **(C)** Group mean data (SEM) for OCT FS at 1 week ($n=13$/group) and 2 weeks ($n=6$–8/group) after transient (3 day) Mito*Xho*I induction. **(D)** Merged confocal analysis of mitochondrial nucleoid content: left, *Drosophila* heart tube is from 1 week control and right, heart tube is from 1 week after transient cardiac-specific Mito*Xho*I expression. Red is mito-tracker red, green is anti-DNA, nuclei are counterstained blue with DAPI. Mitochondrial nucleoids are visible as small yellow/green punctae within red mitochondria. White scale bar is 50 μm. Quantitative data ($n=3$ fly tubes/group) are on the right. FS, fractional shortening; OCT, optical coherence tomography.

heart development and function, but early lethality precluded a more detailed characterization of cardiac phenotypes.

To better understand the time-dependent consequences of cardiomyocyte mtDNA linearization we employed a conditional Gal80ts system (Fig. 5B, left) to induce Mito*Xho*I in the heart tubes of adult flies. Flies were bred and allowed to develop through the pupal stage at 19°C, which does not permit Mito*Xho*I expression. Newly emerged adults were moved to the expression-permissive temperature of 29°C for 3 days, which induced cardiomyocyte transgene expression as measured by an enhanced green fluorescent protein (eGFP) marker driven by the same tincΔ4Gal4/Gal80ts system. One week after Mito*Xho*I induction, *Drosophila* heart tubes exhibited reduced contractility, measured as decreased fractional shortening (%FS), compared with identically treated controls (Fig. 5B, right, C). This is the fruit fly analog of dilated cardiomyopathy (16). To determine the capacity of fruit fly heart tubes to recover from mtDNA linearization by *Xho*I we studied a separate cohort of flies 2 weeks after Mito*Xho*1 induction. Because these flies were placed at the normal maintenance temperature of 23°C after 3 days at the permissive temperature of 29°C, they had 10 days to repair or eliminate the damaged mitochondrial genomes and recover cardiac function. Yet, we observed no functional recovery during this period (Fig. 5C). Cardiomyocyte mtDNA was quantified by confocal analysis of mitochondrial nucleoids, and it was markedly decreased by *Xho*I expression (Fig. 5D). Together, these results indicate that double-strand breaks of mtDNA such as those induced by *Xho*I-mediated linearization are persistent, are sufficient to deplete cardiomyocyte mtDNA, and will lead to cardiomyopathy.

Discussion

Here, in studies of mouse hearts, *Drosophila* heart tubes, and mitochondrial genomes, we detected double-stranded mtDNA breaks after interrupting Mfn2-dependent cardiac mitochondrial quality control. We further demonstrated that mtDNA linearization is sufficient to cause cardiomyopathy. These results reveal deleterious effects of mitochondrial genome linearization, and not just in–del mutations, on mitochondrial homeostasis in the heart.

We tend to conceive of mitochondria as having a life cycle; new mitochondria are formed *via* "biogenesis" (21), they function for a period of time, and then they become senescent, manifested as depolarization and increased production of toxic reactive oxygen species (ROS) (3). Because senescent mitochondria are cytotoxic, fission/fusion and mitophagy mechanisms have evolved to eliminate them. Dysfunctional mitochondria sequester damaged components into one of two daughter mitochondria formed *via* assymetrical organelle fission; the defective daughter mitochondrion is then selectively eliminated *via* mitophagy, whereas the more normal daughter mitochondrion is reintroduced into the cell population *via* fusion (35). Thus, mitochondrial dynamics and mitochondrial quality control are inextricably related. The current results add the genetic program for producing new mitochondrial proteins, or "mitochondrial biogenesis" into this schema, supporting functional integration of mitochondrial dynamics, biogenesis, and quality control.

mtDNA mutations have been implicated in myopathic phenotypes in the "mito-mutator mouse," which expresses a proofreading defective mtDNA polymerase (14), and after combined skeletal muscle ablation of Mfn1 and Mfn2 (8). Using ultra-deep resequencing of mtDNA we did not find evidence that increased mtDNA single-nucleotide mutations contribute to the cardiomyopathy caused by cardiac Mfn2 deletion. We believe that lack of causality of single nucleotide variants in the current study is consistent with a number of prior observations: First, mitochondrial mutations in the mito-mutator and skeletal muscle Mfn1/Mfn2 double knockout mice were associated with mitochondrial respiratory compromise and/or dissipation of mitochondrial inner membrane potential, which were not induced by cardiac Mfn2 deficiency (9, 10). Second, mitochondrial mutations in genes encoding OXPHOS proteins or tRNAs in the mito-mutator mouse undergo trans-generational clonal expansion to produce mitochondrial respiratory dysfunction and increased ROS (1). Because we ablated *mfn2* in cardiac myocytes after embryonic development, mtDNA heritability can play no role in our studies. Third, although mtDNA has a mutation rate 10–20 times higher than nuclear DNA (attributed to absence of protective histones and limited repair mechanisms) (4), the vast majority of mtDNA mutations are functionally recessive (34). Thus, 60%–90% of mtDNAs in heteroplasmic cells can harbor mutations before mitochondrial respiration dysfunction is observed (13, 32).

Mitochondrial abnormalities induced by interruption of PINK1-Parkin signaling after postnatal cardiomyocyte-specific Mfn2 deletion include increased mitochondrial size (9) and a decline in mtDNA content. The progressive cardiomyopathy of Mfn2 deficiency is therefore linked to replacement of normal mitochondria with larger mitochondria having fewer mitochondrial genomes. The ~16.6 kb mitochondrial genome encodes 13 mitochondrial proteins in addition to 22 tRNAs and 2 rRNAs. Transcription of mitochondrial-encoded RNAs is bidirectional on the heavy and light mtDNA chains, and would be interrupted by the double-stranded DNA breaks that we identified. Although in–dels in mtDNA repair the circular genome structure and therefore permit transcription and replication, linearization of mtDNA likely represents a functional dead-end, interrupting mitochondrial replication, which is a critical mitochondrial component of mitochondrial biogenesis (25). We observed that the nuclear mitochondrial biogenesis program increased in apparent compensation.

An individual mitochondrion typically has several copies of its genome packaged as discreet nucleoprotein complexes, or nucleoids, which can be exchanged between fused mitochondria in a form of genetic complementation (30). Mitochondrial fusion mediated by Mfn1, Mfn2, and Opa1 also facilitates exchange of mitochondrial gene products, that is, mtDNA-encoded proteins, tRNAs, and rRNAs. Mixing of mitochondrial inner and outer membranes, nuclear- and mitochondrial-encoded respiratory enzymes, translational and transcriptional machinery, and other matrix components between fused mitochondria temporarily compensates for perturbations of defective genomes, renewing mitochondrial respiratory function. Mitochondria that are excessively damaged, including those with defective genomes, do not undergo fusion-dependent functional complementation and instead are targeted for elimination through the process of mitophagy.

In the context of Mfn2 acting as a critical mediator of PINK1-Parkin signaling and a mitochondrial fusion factor (9,

26, 31, 33), and the current observation that mtDNA levels plummet in Mfn2-deficient cardiomyopathic hearts, we have re-evaluated our concept of a mitochondrial life cycle. As the descendents of primordial bacteria that developed endosymbiotic relationships with ancestral unicellular organisms, we believe that mitochondria have no life cycle *per se*; like the bacteria from which they descended, mitochondria are immortal. Since there are no "newborn" mitochondria, what is the function of the gene expression program we describe as mitochondrial biogenesis? We propose that nuclear and mitochondrial biogenic programs do not supply new organelles, but instead produce replacement components for functioning mitochondria as they endlessly cycle between renewal and senescence. The current studies indicate that Mfn2, acting as the transducer of PINK1-Parkin mitophagy signaling, helps to maintain the integrity of mitochondrial renewal by preventing accumulation of mtDNA with double-stranded breaks. We further demonstrate that mtDNA linearization is sufficient to cause the type of cardiomyopathies that are observed in mice and flies when PINK1-Mfn2-Parkin-mediated mitophagy is interrupted (9). We suggest that linearized mtDNA deserves evaluation as a potential contributing factor in other diseases, like Parkinson's and Alzheimer's disease, in which defects in mitochondrial quality control apparati can be causative.

Materials and Methods

Mouse generation and phenotypic analyses

$Mfn2^{loxp/loxp}$ mice (6, 7) were obtained from University of California-Davis and crossed onto the *Myh6*-nuclear-directed "turbo" Cre line (36) for cardiomyocyte-specific gene deletion after birth. The cardiac phenotype of these mice was described previously (9, 10). All experimental procedures were approved by the Animal Studies Committee at Washington University School of Medicine.

Transcriptional profiling by deep mRNA sequencing of mouse hearts

Transcriptional profiling of Mfn2-KO cardiac tissues was performed by deep mRNA sequencing as described (28). Heat mapping of expression data and statistical analysis used Partek Genomics Suite version 6.4 (Parteko). Original RNA sequence data have been deposited at https://submit.ncbi.nlm.nih.gov/subs/bioproject/, project number SRX285687.

Mouse mitochondrial genomics analyses

Ultra-deep mtDNA sequencing started with isolated cardiac mitochondria. mtDNA was purified using phenol/chloroform extraction and ethanol precipitation. For each heart, 50–100 ng of mtDNA was randomly fragmented by sonication (Diagenode Bioruptor XL). Following column purification (Qiaquick; Qiagen) Illumina sequencing libraries were generated as previously described (28) and single-end sequenced on an Illumina HiSeq. Raw sequence reads (42 nt per read at an average of 67.3 million reads, with 65.3% alignment to the mitochondrial genome) were aligned to the C57BL6/J mitochondrial genome (GenBank: EF108336.1) using Bowtie package version 0.12.7 (24), allowing up to three mismatched nucleotides per read while stipulating that each read align to one genomic position only. VarScan version 2.2.3 (22) was used to calculate coverage depth and call variants from aligned reads, using minimum Illumina nucleotide quality scores of 32. The average coverage depth was >100,000; the lowest coverage depth among the mtDNA samples ~40,000, in which a single sequence variant in a single read would be observed at frequency of 0.000025. Thirty reads were nominated as a minimum for a confident call, resulting in a minimum detectable frequency of 0.00075 that was used for analysis of all samples. Variants that were not observed on both DNA strands were censored (~4% of observed variation). Original mtDNA sequence data have been deposited at https://submit.ncbi.nlm.nih.gov/subs/bioproject/, project number SRX285809.

To compare the amounts of mtDNA and nuclear DNA, we used quantitative PCR (11). Relative copy number differences are expressed as the difference in amplification cycle threshold, $C(t)$, between mtDNA and nuclear DNA assays ($\Delta C(t)$ method).

To detect regional deletions in mtDNA, we designed PCR primers to span regions of CNV detected by mtDNA sequencing. Thermopol Taq DNA polymerase system was used for PCR (94°C 30 s, 60°C 30 s, 72°C 1.5 min): Primer pair 1; forward, 5′ gccaatgaaatgggaagaaa; reverse, 5′ atgccgtatggac caacaat (amplifies mtDNA nucleotide 761–2884). Primer pair 2; forward, 5′ ggcctcacatcatcactcct, reverse, 5′ ctcgtccga catgaaggaat (amplifies mtDNA nucleotide 13163–14720). Primer pair 3 (negative control); forward, 5′ accagcattccagtcctcac, reverse, 5′ tagggccgcgataataaatg (amplifies mtDNA nucleotide 9410–11457).

Linearization of mtDNA was detected by mtDNA -specific southern blotting of total cardiac DNA (2 mg) after size-separation on 0.5% agarose gels (20 h at 60 V). Intact and *Xho*I-digested mouse mtDNA were run as controls.

Mitochondrial nucleoids were visualized in isolated murine cardiomyocytes or *Drosophila* heart tubes by merged confocal microscopy of mitochondria (MitoTracker Red) and DNA (anti-dsDNA, #ab27156; Abcam) and quantified using ImageJ.

Drosophila *lines and cardiac analyses*

Drosophila melanogaster tub-Gal80ts; tinCΔ4-Gal4 (obtained from Rolf Bodmer, Sanford-Burnham Medical Research Institute) were crossed to UASp-Mito*Xho*I 2.1/CyO (provided by Patrick O'Farrell, UCSF) to generate F1 progeny with temperature-inducible cardiomyocyte-specific expression of Mito*Xho*I. Parental crosses were maintained at 19°C, which does not permit transgene expression. Emerging F1 progeny were collected each day and incubated at 29°C for 3 days for transgene induction, and then shifted to room temperature for maintenance (22–23°C). Expression characteristics of the tub-Gal80ts; tinCΔ4-Gal4 system as a function of these temperatures were monitored with UASp-eGFP (Bloomington stock #6874). Heart tube contraction was assessed using OCT as described (16, 18) at room temperature on 7- and 14-day-old flies. Control crosses were set up with w^{1118} (Bloomington stock #6326).

Statistical methods

Data are presented as mean ± SEM, except for average mtDNA sequence depth that is depicted as mean ± SD. Paired comparisons between Mfn2-deficient hearts and their age-

matched controls used Student's *t*-test. Multiple comparisons for mtDNA mutation analyses, in which 6 and 16 week controls were pooled, used one-way ANOVA and Newman–Keuls test, or Kruskal–Wallis tests for nonparametric data. Differences in data distribution were examined using Chi-square test. Statistical difference was defined as $p < 0.05$. RNA-sequence expression data were analyzed at an FDR of 0.01; *p*-values comparing expression levels of all ~1100 regulated mRNAs in 6- and 16-week-old Mfn2-deficient hearts to their age-matched controls are in Supplementary Table S1. GO category assignment and over-representation used BiNGO.

Acknowledgment

Supported in part by NIH grants HL59888 and HL107276.

Author Disclosure Statement

No competing financial interests exist.

References

1. Ameur A, Stewart JB, Freyer C, Hagstrom E, Ingman M, Larsson NG, and Gyllensten U. Ultra-deep sequencing of mouse mitochondrial DNA: mutational patterns and their origins. *PLoS Genet* 7: e1002028, 2011.
2. Ashley MV and Willis CJ. Analysis of mitochondrial DNA polymorphisms among Channel Island deer mice. *Evolution* 41: 854–863, 1987.
3. Bratic A and Larsson NG. The role of mitochondria in aging. *J Clin Invest* 123: 951–957, 2013.
4. Brown WM, George M Jr., and Wilson AC. Rapid evolution of animal mitochondrial DNA. *Proc Natl Acad Sci USA* 76: 1967–1971, 1979.
5. Chan DC. Fusion and fission: interlinked processes critical for mitochondrial health. *Annu Rev Genet* 46: 265–287, 2012.
6. Chen H, Detmer SA, Ewald AJ, Griffin EE, Fraser SE, and Chan DC. Mitofusins Mfn1 and Mfn2 coordinately regulate mitochondrial fusion and are essential for embryonic development. *J Cell Biol* 160: 189–200, 2003.
7. Chen H, McCaffery JM, and Chan DC. Mitochondrial fusion protects against neurodegeneration in the cerebellum. *Cell* 130: 548–562, 2007.
8. Chen H, Vermulst M, Wang YE, Chomyn A, Prolla TA, McCaffery JM, and Chan DC. Mitochondrial fusion is required for mtDNA stability in skeletal muscle and tolerance of mtDNA mutations. *Cell* 141: 280–289, 2010.
9. Chen Y and Dorn GW 2nd. PINK1-phosphorylated mitofusin 2 is a Parkin receptor for culling damaged mitochondria. *Science* 340: 471–475, 2013.
10. Chen Y, Csordas G, Jowdy C, Schneider TG, Csordas N, Wang W, Liu Y, Kohlhaas M, Meiser M, Bergem S, Nerbonne JM, Dorn GW 2nd, and Maack C. Mitofusin 2-containing mitochondrial-reticular microdomains direct rapid cardiomyocyte bioenergetic responses *via* interorganelle Ca2+ crosstalk. *Circ Res* 111: 863–875, 2012.
11. Chen Y, Lewis W, Diwan A, Cheng EH, Matkovich SJ, and Dorn GW 2nd. Dual autonomous mitochondrial cell death pathways are activated by Nix/BNip3L and induce cardiomyopathy. *Proc Natl Acad Sci USA* 107: 9035–9042, 2010.
12. Chen Y, Liu Y, and Dorn GW 2nd. Mitochondrial fusion is essential for organelle function and cardiac homeostasis. *Circ Res* 109: 1327–1331, 2011.
13. Chomyn A. The myoclonic epilepsy and ragged-red fiber mutation provides new insights into human mitochondrial function and genetics. *Am J Hum Genet* 62: 745–751, 1998.
14. Dai DF, Chen T, Wanagat J, Laflamme M, Marcinek DJ, Emond MJ, Ngo CP, Prolla TA, and Rabinovitch PS. Age-dependent cardiomyopathy in mitochondrial mutator mice is attenuated by overexpression of catalase targeted to mitochondria. *Aging Cell* 9: 536–544, 2010.
15. Dorn GW 2nd. Mitochondrial dynamics in heart disease. *Biochim Biophys Acta* 1833: 233–241, 2013.
16. Dorn GW 2nd, Clark CF, Eschenbacher WH, Kang MY, Engelhard JT, Warner SJ, Matkovich SJ, and Jowdy CC. MARF and Opa1 control mitochondrial and cardiac function in *Drosophila*. *Circ Res* 108: 12–17, 2011.
17. Dorn GW 2nd, Robbins J, and Sugden PH. Phenotyping hypertrophy: eschew obfuscation. *Circ Res* 92: 1171–1175, 2003.
18. Eschenbacher WH, Song M, Chen Y, Bhandari P, Zhao P, Jowdy CC, Engelhard JT, and Dorn GW 2nd. Two rare human mitofusin 2 mutations alter mitochondrial dynamics and induce retinal and cardiac pathology in *Drosophila*. *PloS One* 7: e44296, 2012.
19. Gerhold JM, Aun A, Sedman T, Joers P, and Sedman J. Strand invasion structures in the inverted repeat of Candida albicans mitochondrial DNA reveal a role for homologous recombination in replication. *Mol Cell* 39: 851–861, 2010.
20. Kelly DP. Cell biology: ageing theories unified. *Nature* 470: 342–343, 2011.
21. Kelly DP and Scarpulla RC. Transcriptional regulatory circuits controlling mitochondrial biogenesis and function. *Genes Dev* 18: 357–368, 2004.
22. Koboldt DC, Chen K, Wylie T, Larson DE, McLellan MD, Mardis ER, Weinstock GM, Wilson RK, and Ding L. VarScan: variant detection in massively parallel sequencing of individual and pooled samples. *Bioinformatics* 25: 2283–2285, 2009.
23. Kowald A and Kirkwood TB. Mitochondrial mutations and aging: random drift is insufficient to explain the accumulation of mitochondrial deletion mutants in short-lived animals. *Aging Cell* 12: 728–731, 2013.
24. Langmead B, Trapnell C, Pop M, and Salzberg SL. Ultrafast and memory-efficient alignment of short DNA sequences to the human genome. *Genome Biol* 10: R25, 2009.
25. Lecrenier N and Foury F. New features of mitochondrial DNA replication system in yeast and man. *Gene* 246: 37–48, 2000.
26. Lee S, Sterky FH, Mourier A, Terzioglu M, Cullheim S, Olson L, and Larsson NG. Mitofusin 2 is necessary for striatal axonal projections of midbrain dopamine neurons. *Hum Mol Genet* 21: 4827–4835, 2012.
27. Lipinski KA, Kaniak-Golik A, and Golik P. Maintenance and expression of the *S. cerevisiae* mitochondrial genome—from genetics to evolution and systems biology. *Biochim Biophys Acta* 1797: 1086–1098, 2010.
28. Matkovich SJ, Zhang Y, Van Booven DJ, and Dorn GW 2nd. Deep mRNA sequencing for *in vivo* functional analysis of cardiac transcriptional regulators: application to Galphaq. *Circ Res* 106: 1459–1467, 2010.
29. Negritto MC. Repairing double-strand DNA breaks. *Nat Educ* 3: 26, 2010.
30. Ono T, Isobe K, Nakada K, and Hayashi JI. Human cells are protected from mitochondrial dysfunction by complemen-

tation of DNA products in fused mitochondria. *Nat Genet* 28: 272–275, 2001.
31. Pham AH, Meng S, Chu QN, and Chan DC. Loss of Mfn2 results in progressive, retrograde degeneration of dopaminergic neurons in the nigrostriatal circuit. *Hum Mol Genet* 21: 4817–4826, 2012.
32. Rossignol R, Faustin B, Rocher C, Malgat M, Mazat JP, and Letellier T. Mitochondrial threshold effects. *Biochem J* 370: 751–762, 2003.
33. Sebastian D, Hernandez-Alvarez MI, Segales J, Sorianello E, Munoz JP, Sala D, Waget A, Liesa M, Paz JC, Gopalacharyulu P, Oresic M, Pich S, Burcelin R, Palacin M, and Zorzano A. Mitofusin 2 (Mfn2) links mitochondrial and endoplasmic reticulum function with insulin signaling and is essential for normal glucose homeostasis. *Proc Natl Acad Sci USA* 109: 5523–5528, 2012.
34. Taylor RW and Turnbull DM. Mitochondrial DNA mutations in human disease. *Nat Rev Genet* 6: 389–402, 2005.
35. Twig G and Shirihai OS. The interplay between mitochondrial dynamics and mitophagy. *Antioxid Redox Signal* 14: 1939–1951, 2011.
36. van Berlo JH, Elrod JW, van den Hoogenhof MM, York AJ, Aronow BJ, Duncan SA, and Molkentin JD. The transcription factor GATA-6 regulates pathological cardiac hypertrophy. *Circ Res* 107: 1032–1040, 2010.
37. Williams SL, Huang J, Edwards YJ, Ulloa RH, Dillon LM, Prolla TA, Vance JM, Moraes CT, and Zuchner S. The mtDNA mutation spectrum of the progeroid Polg mutator mouse includes abundant control region multimers. *Cell Metab* 12: 675–682, 2010.
38. Xu H, DeLuca SZ, and O'Farrell PH. Manipulating the metazoan mitochondrial genome with targeted restriction enzymes. *Science* 321: 575–577, 2008.
39. Youle RJ and van der Bliek AM. Mitochondrial fission, fusion, and stress. *Science* 337: 1062–1065, 2012.
40. Zechner C, Lai L, Zechner JF, Geng T, Yan Z, Rumsey JW, Collia D, Chen Z, Wozniak DF, Leone TC, and Kelly DP. Total skeletal muscle PGC-1 deficiency uncouples mitochondrial derangements from fiber type determination and insulin sensitivity. *Cell Metab* 12: 633–642, 2010.

Address correspondence to:
Prof. Gerald W. Dorn II
Department of Internal Medicine
Center for Pharmacogenomics
Washington University School of Medicine
660 S. Euclid Ave., Campus Box 8220
St. Louis, MO 63110

E-mail: gdorn@dom.wustl.edu

Date of first submission to ARS Central, May 16, 2013; date of final revised submission, July 18, 2013; date of acceptance, August 2, 2013.

Abbreviations Used

CNV = copy number variation
eGFP = enhanced green fluorescent protein
FDA = false discovery rate
FS = fractional shortening
in–del = insertion-deletion
Mfn = mitofusin
mtDNA = mitochondrial DNA
OCT = optical coherence tomography
PCR = polymerase chain reaction
PINK1 = PTEN-induced putative kinase 1
rRNA = ribosomal RNA
ROS = reactive oxygen species
SD = standard deviation
tRNA = transfer RNA